


A Cost-Efficient FOC-controlled Haptic Knob for Industrial Robot Programming with Force Feedback

Junsheng Ding^{*†} 

Xiangyu Fu^{*†} 

Tiantian Wei^{*†} 

Alexander Perzylo^{*†} 

Abstract—Robot programming is still an elaborate process in industrial assembly, especially in cases requiring a specific force profile for successfully executing an assembly step. In this work, we present the Haptic Knob, a low-cost haptic device (around 100 EUR on hardware costs) for (currently) one-dimensional robot movement programming on both position and force profiles. The Haptic Knob is equipped with a Field-Oriented Controlled (FOC) motor and a positional encoder that reads the human input position and generates feedback forces to the operator. The Haptic Knob is not equipped with an external Force/Torque sensor to measure the human input force, but works together with the impedance controller of the robot arm, which allows a dynamic force teach-in. A control interface is implemented to map the positional signal from the Haptic Knob to the movement of different actuators, as well as the force/torque signals from various devices to the Haptic Knob for force feedback. We showcase and validate the proposed hardware and control interface on the industrial use case of automotive fuse box assembly.

Index Terms—Haptic device, force feedback, robot teleoperation

I. INTRODUCTION

Classical robot programming using the teach pendant, such as the KUKA smartPad¹ is still widely used in the industrial, where the operator defines a sequence of way-points in the Cartesian space for the robot movement. While the teach pendant enables the precise control of the robot’s Tool Center Point (TCP), it is an elaborate process where the operator has to finetune the final robot pose under sub-millimeter accuracy with only visual feedback, which makes it less efficient. Moreover, this method only allows for the programming of the way-points of the robot movement but neglects the teaching of force profiles, which are crucial for certain industrial assembly tasks, such as the insertion of fragile workpieces with a specific force threshold.

Haptic teleportation devices, such as Virtuose 6D HF TAO², sigma.7³ and Touch⁴, allows the human operator to precisely control the robot’s movement with haptic force feedback [1]. During the haptic teleoperation, the operator’s movements on the devices are directly mapped onto the Cartesian movement

^{*}J. Ding, X. Fu, T. Wei, A. Perzylo are with fortiss, Research Institute of the Free State of Bavaria associated with Technical University of Munich, Germany. Please direct all correspondence to ding@fortiss.org.

[†]Equal contribution

¹<https://www.kuka.com/en-de/products/robot-systems/robot-controllers/smartpad>

²<https://www.haption.com/robotics/products-1>

³<https://www.forcedimension.com/products/sigma>

⁴<https://www.3dsystems.com/haptics-devices/touch>

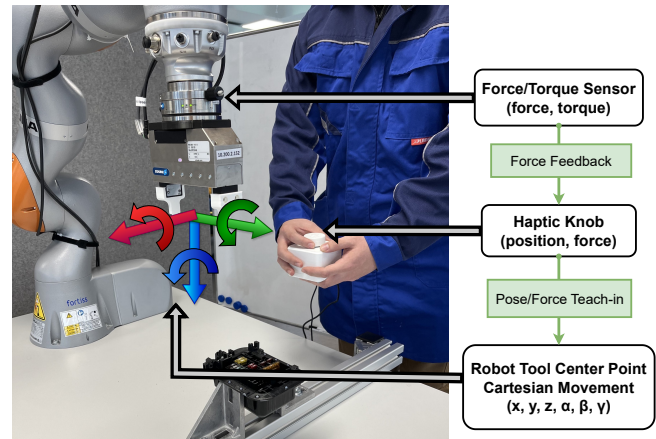


Fig. 1: Our proposed haptic device for one-dimensional (1D) robot teach-in on both position and force. The contact force on the robot end effector (EE) is fed back to the human operator for precise force control.

of the robot’s TCP. These devices are particularly efficient for robot teach-in or teleoperation [2]–[5], where the force profile of the robot movement is crucial, e.g. assembly tasks of fragile workpieces or polishing tasks. The appropriate force feedback on the operator requires actuators with larger sizes, which result in a less compact hardware dimension, further limiting their applications in industrial settings. Additionally, the force feedback of these devices is enabled with high-precision Force/Torque (F/T) sensors and actuators, resulting in high costs that limit their wide adoption in the industry.

Field Oriented Controller (FOC) [6] allows for the precise control of the motor’s position and torque, which makes it potentially suitable for force feedback within a haptic device. Our work is motivated by the Smart Knob project⁵ [7], where the FOC controller is used for intuitive user input with haptic feedback, e.g. for controlling smart home devices. However, the haptic feedback of such Smart Knob is currently limited in simulating detents or controlling boundaries, which is not directly linked to the interaction force with the physical objects. To our best knowledge, such devices have not been presented as haptic teleoperation interfaces for robot control, particularly for physical interaction with real-world objects. In this work, we propose a low-cost FOC-controlled Haptic Knob

⁵<https://github.com/scottbez1/smartknob>

(around 100 EUR on hardware costs) and the necessary control framework for robot teleoperation. In addition, we investigate and showcase the usability of such devices with an industrial assembly task with force requirement.

The paper is structured as follows: In section II, we give a literature overview on the current haptic teleoperation devices with their industrial use cases. In section III, we introduce the implemented system, including the hardware design of the Haptic Knob III-A, and the software design of the control interface III-B. In addition, we introduce the design of the robot controller as an example of force teach-in. In section IV, we showcase the usability of the Haptic Knob in an industrial setting for automotive fuse box assembly task as the experiment and further present and discuss the result results in section V.

II. RELATED WORKS

Robot Teaching with force requirements: Force requirements on robot movements are crucial in certain industrial tasks involving delicate manipulations, such as the assembly of small electrical parts [8] or polishing [9]. Kinesthetic teaching has emerged as a viable method for enabling robots to learn both position and force profiles in various industrial use cases [9]–[11]. During kinesthetic teaching, a user physically guides a robot along the necessary trajectories to complete a task. This hands-on approach is more intuitive than the classical teach-pendant approach. However, the kinesthetic teaching necessitates the direct physical interaction of the operator with the robot arm, which may result in safety risks due to robots’ malfunctions. In comparison, haptic devices allow for the teaching of positional and force requirements with the additional advantage of safer remote control [3], [10], [12].

Haptic Teleoperation: Compared to Kinesthetic teaching, robot teleoperation enables a human operator to control a robot remotely with rich haptic feedback, which allows the operator to perceive and respond to the robot’s environment intuitively and precisely. Different studies utilize the haptic feedback in various robot manipulation tasks, including the peg-in-hole [2], [3], the pipe-fitting [5], the bimanual cloth-folding [13], the cutting task [4], and the blackboard writing task [14].

The force teach-in with the haptic device can be integrated with an impedance controller on the actuator side to allow more dynamic force manipulation. Michel et al. [4] introduced an adaptive impedance controller on robot teleoperation with the Omega.3 haptic device, where the task execution is improved with the dynamic force from the adaptive stiffness parameter. Similarly, we deploy an impedance controller on the robot side for dynamic force teach-in.

More recently, haptic devices have been utilized for data collection of robot manipulation in imitation learning [12], [13]. Chi et al. [13] utilized two Haption Virtuose 6D HF TAO to demonstrate complex and contact-rich tasks on the robot arm, e.g. bimanual shirt folding task, where the robot learns the subtle manipulation policy from hundreds of human demonstrations.

Haptic Feedback Devices: Despite the recent advances in haptic teleportation, existing haptic devices often face trade-offs between compact size and accurate force feedback [1].

The current haptic devices mostly interact with 2 sensory modalities of the human [15]: (1) Cutaneous sensation (also known as tactile sensation) enables the perception of pressure, shear, and vibration through the skin [15], that allows the detection of objects attributes of shape, texture, and edges [16]; (2) Kinesthetic sensations, in contrast, provide feedback on forces and torques, informing the body’s position and movement.

Cutaneous feedback devices are more compact and portable, making them suitable for wearable devices [17], [18]. However, they do not facilitate position or force teaching. In contrast, kinesthetic feedback devices designed for position and force teaching, such as the sigma.7 used in [19], are typically mechanical and grounded. These devices are often expensive and bulky, limiting their portability and making integration into diverse industrial settings more challenging [20]. Our proposed device, however, facilitates both force and position teaching while maintaining portability and cost-efficiency due to its compact hardware design.

III. METHOD

Our proposed method for intuitive robot teaching includes 3 major components as depicted in Fig. 2: (1) A FOC-controlled Haptic Knob (on the right) as the master device during the teleoperation that reads the user’s positional input and returns force feedback; (2) A control interface (in the middle) that maps the feedforward position value and feedback force value between the Haptic Knob and the robotic devices; (3) The devices (on the left) within the robot workcell that either serve as the slave device, e.g., robot arms, or measure the force/torque value, e.g., F/T sensors.

During the robot teach-in, the human operator can hold the portable Haptic Knob in hand and rotate the motor in circles. The Haptic Knob is a one-dimensional (1D) teleoperation device, that allows for switching between different teleoperation channels due to its hardware-agnostic property, e.g. position control on the Cartesian movement along the Z axis of the robot’s TCP P^{TCP_Z} and the correspondent force feedback F^{TCP_Z} as in our use case IV. The user’s rotational input on the Haptic Knob is measured by a rotational encoder as $P^{HapticKnob}$. The control interface reads the change of the motor $\Delta P^{HapticKnob}$ and further converts it into a 1D relative movement $\Delta P^{Actuator}$ command on the actuators, e.g. ΔP^{TCP_Z} as in our use case. For force feedback control, the contact force on the actuators with the external objects can be measured via F/T sensors as F^{Sensor} , which is also a one-dimensional value, e.g. F^{TCP_Z} . The F^{Sensor} is also converted to torque command $T^{HapticKnob}$ on the Haptic Knob for force feedback. The exerted torque on the Haptic Knob can be perceived by the human hand. All components within our system are wrapped in a Robot Operating System (ROS) interface to allow unified data communication with ROS messages.

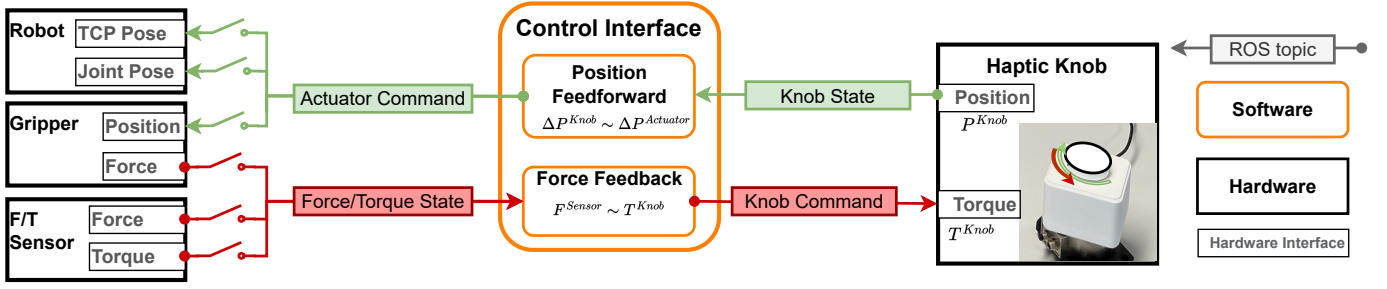


Fig. 2: System architecture of our proposed haptic control method. The haptic knob is a hardware-agnostic device for 1D position and force teach-in. A control interface in the center is responsible for converting the position and force signals between the Haptic Knob and other devices: (1) forward position teach-in from the haptic knob to the actuators, e.g. Cartesian movement on the Z axis of robot TCP; (2) Force feedback control from the sensors, e.g. F/T sensor installed on the robot EE, to the haptic knob as the haptic feedback for human operator.

In the following sections, we explain the working principle and the functionality of each component. In Section III-A, we first give a brief recap on the FOC controller and also introduce the hardware and software design of the Haptic Knob, which explains why it can be used for haptic position control; In Section III-B, we explain the linear mapping of the device signals within our control interface that enable the positional feedforward and force feedback teleoperation. In Section III-C, we introduce specifically the deployment of a Cartesian impedance controller on the robot as an example of the dynamic force teach-in.

A. FOC-based Haptic Knob

The hardware components within our proposed Haptic Knob are depicted in Fig. 3. Field-Oriented Control (FOC) is the key technology for controlling the torque on a brushless DC (BLDC) motor and reading the positional value of the motor’s rotation. We utilize a compact BLDC motor⁶ with a maximal torque of 0.124Nm, which is typically used in drones or gimbals. The measurement of the motor’s position is enabled by a magnetic encoder AS5600⁷ with the resolution of 4096 units per circle, i.e. $1.534 \times 10^{-3} \text{rad/unit}$. The acquired motor position is also used for measuring the human input. We implemented a FOC controller based on the SimpleFOC library [7], integrated into an ESP32 microcontroller. In addition, rosserial⁸ is integrated into the ESP32 to allow data transmission via ROS, enabling commands on the Haptic Knob’s force and publication of the motor’s position.

Figure 4 shows the block diagram of our FOC controller, where efficient and precise motor control is fundamental for realistic haptic feedback. FOC [6] utilizes the Park and Clarke Transformation for decomposing a user-specified voltage value U_q set by the user into two orthogonal components (i_{sd} and i_{sq}) that align with the rotor’s magnetic field [21]. It then adjusts the phase voltages U_a , U_b and U_c to ensure these generate a magnetic force that is always orthogonal to the

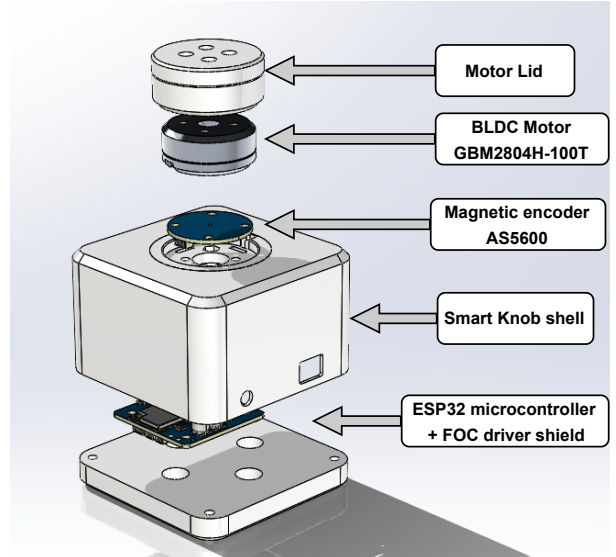


Fig. 3: Exploded view of our proposed Haptic Knob with the hardware components. A BLDC motor is controlled via the FOC driver shield to provide force feedback. The AS5600 encoder is used to measure the rotational position of the motor. An ESP32 microcontroller is integrated into the FOC driver shield to allow communication via ROS. The motor lid, the case, and the base are self-designed and 3D printed.

direction of the rotor’s permanent magnetic field, which allows for the maximal torque through optimal commutation.

For realistic force feedback, a proportional linear relationship between the commanded force and the generated torque on the motor is desired. We first consider the negligible back electromotive force (EMF) that linearly transforms the commanded force to the controlling voltage U_q . Furthermore, FOC enables the proportional linear relationship $T \propto I \propto U_q$ by precisely aligning the stator current vector I with the rotor magnetic field, allowing direct control over torque T , which in turn is directly influenced by the applied voltage U_q . This precise control of the FOC controller is fundamental for capturing the position input from the human operator and

⁶<https://shop.iflight.com/gimbal-motors-cat44/ipower-gm2804-gimbal-motor-pro1153>

⁷<https://ams.com/as5600>

⁸<https://wiki.ros.org/rosserial>

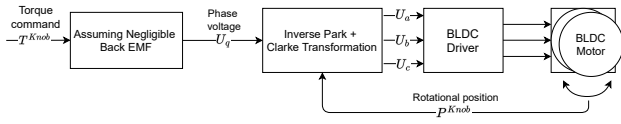


Fig. 4: Block diagram of the FOC-controller for a BLDC motor within our Haptic Knob. The controller takes a force command as system input, which is linearly proportional to the user-defined voltage U_q , considering negligible back EMF for simplification. U_q is further decomposed into phase voltages U_a, U_b, U_c using inverse Park and Clarke Transformation. The optimal magnetic force is ensured by reading the current motor's rotational position. The FOC controller enables precise position and torque control of the motor, which is essential for simulating realistic force feedback.

providing realistic force feedback, thus enhancing the haptic experience by closely imitating real-world forces.

B. Control interface

The control interface, as depicted in the middle of Fig. 2, serves the major purpose of mapping the position/force signal between the Haptic Knob and the workcell devices. Here, we deploy two simple linear mappings on the position/force value between the master and slave devices as expressed in Equations 1 and 2.

The user's input on the Haptic Knob is a rotational position $P^{Haptic Knob}$, which is measured by the magnetic encoder as shown in Fig. 3. To avoid sudden, unsafe robot movement due to inaccuracies in positional readings on the Haptic Knob, the change of the rotational position $\Delta P^{Haptic Knob}$ within each communication iteration is calculated and converted to the change of actuator movement $\Delta P^{Actuator}$ by multiplying a scaling coefficient $K^{Position}$, as expressed:

$$\Delta P^{Actuator} = K^{Position} \times \Delta P^{Haptic Knob} \quad (1)$$

For example, when the Haptic Knob is used for controlling the translational movement on the Z-axis of the robot TCP $P^{TCP Z}$, the $K^{Position}$ is chosen as 0.1 mm/unit assures precise control, which converts the motor's rotation of 360° to the robot TCP movement for 409.6 mm.

The force feedback is also enabled by a coefficient K^{Force} , which linearly maps the force measured on the sensor to torque exerted on the Haptic Knob:

$$T^{Haptic Knob} = K^{Force} \times F^{Sensor} \quad (2)$$

Given the same example of controlling the Z-axis movement of the robot TCP, the K^{Force} is chosen here adequately as $2.5 \times 10^{-3} Nm/N$. When the F/T sensor on the robot TCP detects a collision force of 40 N, the Haptic Knob generates a torque of 0.1 Nm on the user's hand.

The Haptic Knob is a hardware-agnostic device for one-dimensional controlling as in Fig. 2, including the translational or rotational movement of the robot TCP, or the grasping aperture of the gripper. Each controlling mode consists of a

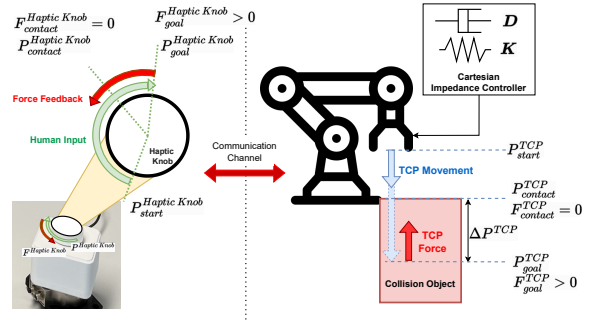


Fig. 5: Illustration of force teach-in of robot movement enabled by a Cartesian impedance controller. The human operator rotates the Haptic Knob to move the robot. Upon collision of robot TCP with objects, the user can still overcome the feedback force on the knob and rotate further to command the next goal position. Due to the increased positional error ΔP^{TCP} , the impedance controller commands the robot movement with a larger force.

1D movement of the actuator and a 1D F/T value from the sensor, with their controlling coefficients manually finetuned for the specific devices.

C. Robot controller

In Figure 5, the process of the force teach-in of the robot movement is illustrated, where the user actively overcomes the current force feedback on the Haptic Knob and commands the next waypoint upon collision. To achieve a low-budget and compact design, the Haptic Knob is not equipped with a F/T sensor to measure the human input force. Instead, the force teach-in is facilitated through an impedance controller [22] in the Cartesian space of the robot TCP. The impedance controller offers the spring-damper characteristic on the robot TCP as expressed in Equation 3, enabling the dynamic force generation upon external collision.

$$\mathcal{F} = K_x(x_d - x) + D_x(\dot{x}_d - \dot{x}) + \hat{\Lambda}(q)\ddot{x}_d + \hat{\mu}(q, \dot{q}) + \hat{\gamma}(q) + \hat{\eta}(q, \dot{q}) \quad (3)$$

Here, \mathcal{F} denotes the external force acting on the robot TCP, which is affected by the difference on the desired position x_d or the velocity \dot{x}_d with the correspondent stiffness and damping factors K_x, D_x . $\hat{\Lambda}, \hat{\mu}, \hat{\gamma}$, and $\hat{\eta}$ represent the robot mechanical model. In our system, the KUKA Fast Research Interface (FRI) offers the Cartesian impedance controller, allowing users to define the damping and stiffness parameters.

During the force teach-in process as in the given example, the robot follows the human's positional moving command. It descends along the Z-axis to the contact point $P^{TCP contact}$ on a collision object. In this contact position, no external force is registered or fed back to the Smart Knob. Subsequently, when the human further commands the next waypoint $P^{TCP goal}$, the robot remains at the contact position $P^{TCP contact}$. The positional

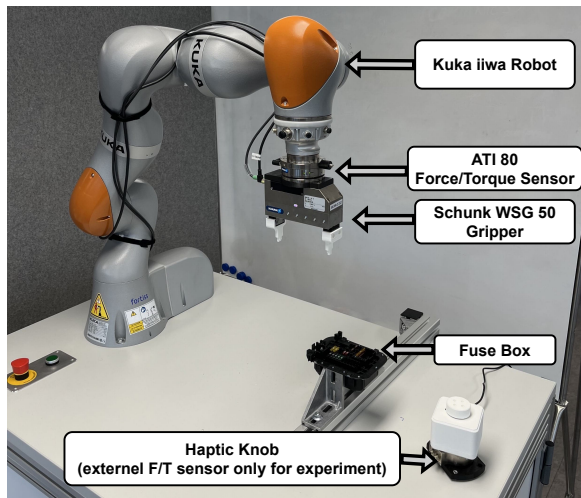


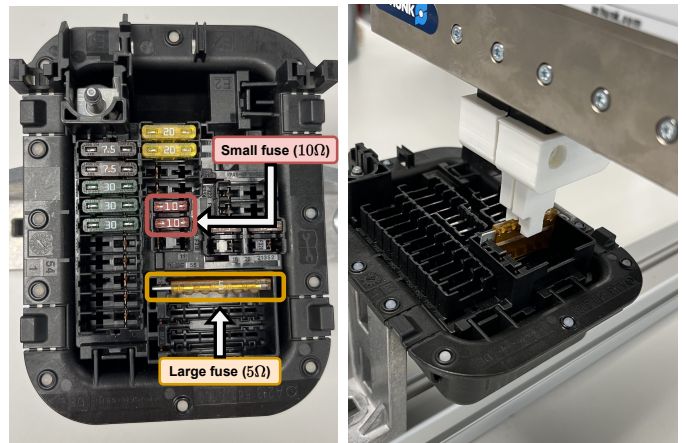
Fig. 6: The hardware setting of the robot workcell for automotive fusebox assembly as the industrial use-case. An external F/T sensor is installed under the Haptic Knob for measurement of the exerted force on the human hand, which is only used during the experiment.

error ΔP^{TCP} between the goal position P_{goal}^{TCP} and the actual position $P_{contact}^{TCP}$ resulted in a contact force on the robot TCP F^{TCP} due to the stiffness characteristic K_x of the impedance controller. This force F_{goal}^{TCP} is measured with a F/T sensor installed on the robot end effector (EE) and fed back to the Haptic Knob. The user can overcome the current force feedback $T^{Haptic Knob}$ and further rotate the Haptic Knob before the upper threshold of the torque on the motor of the Haptic Knob is reached. Due to the stiffness characteristic of the impedance controller, the increasing ΔP^{TCP} results in a larger force F_{goal}^{TCP} applied on the robot. Through this dynamic process, the force profile of the robot TCP movement can be taught by the user.

IV. EXPERIMENTS

To demonstrate the robot force and position teach-in with our Haptic Knob, we choose the automotive fuse box assembly as the use case for the experiment and set up a workcell that closely replicates the real industrial assembly scenario as shown in Fig. 6. The automotive fuse box, as shown in Fig- 7a, possesses many slots, where different types of fuses can be inserted, e.g., large orange fuse 5Ω and small red fuse 10Ω .

The robot movement during each insertion process of a single fuse as shown in Fig. 7b is approximately 5 mm, where applied push-down force is critical for the successful installation. This insertion force has to overcome the resistance in the slot, but exceeding the maximal threshold $F^{Threshold}$ would cause damage to the slot. Such force threshold is difficult to obtain from traditional robot teaching devices, e.g. the teaching pedant, which only allows the user to command the position. Another factor that complicates the robot teaching in this particular use case is the large variation of the fuse



(a) Automotive fuse box (b) Fuse insertion process

Fig. 7: A close-up look on the automotive fusebox (left) for the assembly process. Fuses in different shapes can be inserted into the trays that require different force thresholds, e.g. the small (in shape) red fuse (10Ω) in the middle of the fuse box and the large orange fuse (5Ω) at the bottom right.

types, each requiring a unique force threshold due to their shape differences.

Within the workcell, a KUKA LBR iiwa 7 R800 robot arm is equipped with an AXIA 80 F/T sensor for TCP force measurement and a SCHUNK WSG 50 parallel gripper as the end-effector. The robot arm is internally controlled via the KUKA FRI with a Cartesian impedance controller, which communicates with the controlling PC at a controlling frequency of 1000 Hz and is wrapped with a ROS interface, which allows communication with other components on 500 Hz, enabling real-time capability. The impedance controller is activated with the stiffness parameters of [2000 N/m, 2000 N/m, 2000 N/m, 600 Nm/rad, 600 Nm/rad, 600 Nm/rad] and the damping parameters of [500 Ns/m, 500 Ns/m, 500 Ns/m, 200 Nms/rad, 200 Nms/rad, 200Nms/rad] on the 6 degree of freedom (DOF)[$x, y, z, \alpha, \beta, \gamma$] of the robot TCP.

The fuse box is installed and held on the aluminum profile on the table with a fixed position for the fuse insertion. Two types of fuses (a small red fuse 10Ω and a large orange fuse 5Ω) as in Fig. 7b) are used to illustrate different force profiles. During the experiment, the human operator uses the Haptic Knob to control the Cartesian movement on the Z axis of the robot TCP for the fuse insertion. In order to measure the actual force input of the human operator and compare it with the commanded force on the Haptic Knob, an external Weiss Robotics KMS 40 F/T sensor is installed under the Haptic Knob, which is only used during experiment and is not needed in normal operation. Within each insertion process, the human input of the position $P^{Haptic Knob}$ and the torque exerted $T^{Haptic Knob}$ from the Haptic Knob, as well as the position P^{TCP} and external force F^{TCP} of the robot TCP, are recorded and further analyzed in V.

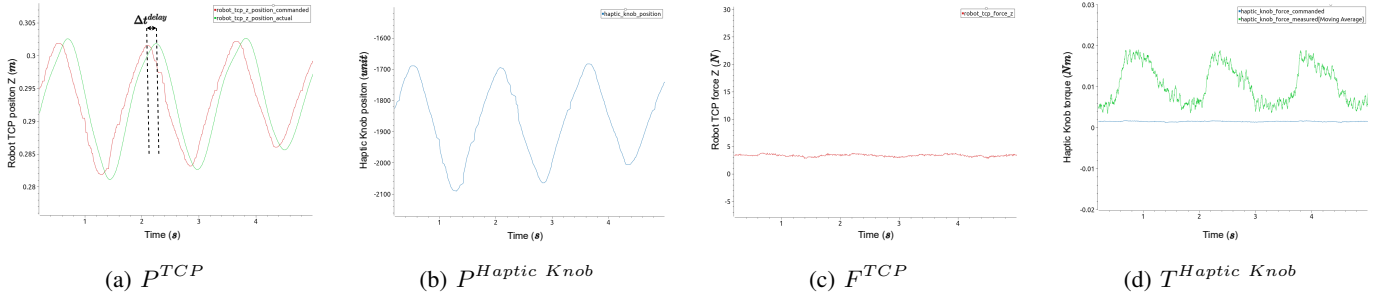


Fig. 8: Experiment result of the collision-free movement of the robot, where the human simulates a sine signal in Fig. 8b. The temporal delay Δt_{delay} on the robot TCP movement in Fig. 8a is caused by the damping characteristic of the Cartesian impedance controller. The disturbance on the measured force on the Haptic Knob in Fig. 8d is caused by the alternating input direction from the human, where no external force is detected on the robot TCP in Fig. 8c.

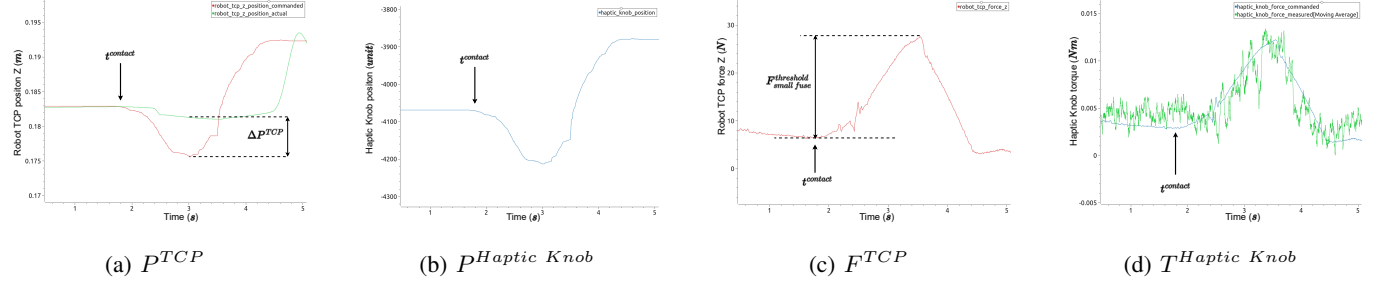


Fig. 9: Experiment result of the insertion process of a small electric fuse requiring low push-down force. The insertion force of $30N$ can be read from in Fig. 9c.

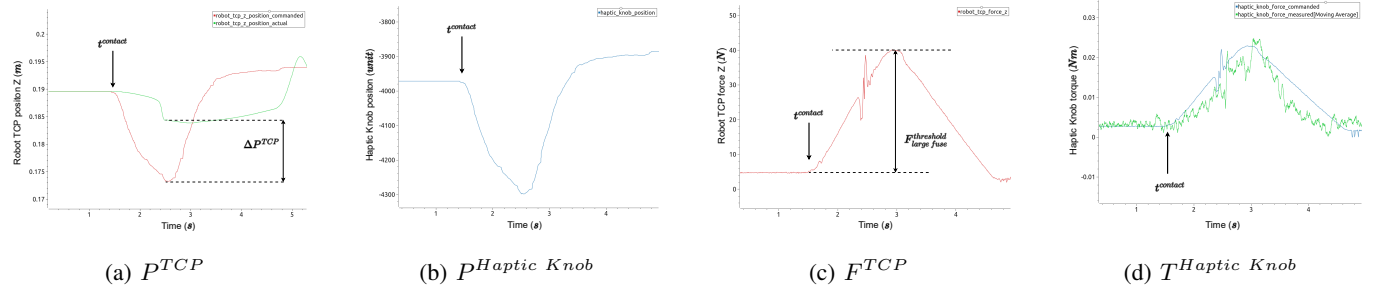


Fig. 10: Experiment result of the insertion process of a large electric fuse requiring high push-down force. The insertion force of $40N$ can be read from in Fig. 10c.

V. RESULTS

A total of 3 different experiments for robot movement teach-in are conducted: (1) a free drive process where the operator simulates a sine signal along the Z-axis of the robot TCP; (2) the insertion process of a small fuse requiring a small push-down force; (3) the insertion process of a large fuse requiring large push-down force. The force and position values of the robot and the Haptic Knob during the 3 experiments are shown as in Fig. 8, 9 and 10

In the free drive experiment, the robot arm follows a sine positional pattern in Fig. 8a that is simulated by the user as shown in Fig. 8b. An average time delay Δt_{delay} of 0.1s between the commanded and the actual robot position is caused by the damping characteristic D from the Cartesian impedance controller, which however leads to a smoother robot movement. Due to the contact-free movement of the robot, no force profile is required as shown in Fig. 8c. Since our Haptic Knob is not a grounded device, the force mea-

surement on it can be inaccurate due to the hand movement. For example, in Fig. 8d, the alternating rotation direction of the human input on the Haptic Knob resulted in a disturbance on the measured force from the external F/T sensor, which, however, does not affect the robot's contact-free movement. Such disturbance of measured force also appeared in the following 2 experiments as shown in Fig. 9d and 10d.

In both fuse insertion experiments, the insertion movement can be successfully taught to the robot from the human as shown in Fig. 9 and 10. The robot's position profiles in both experiments are similar but have different positional errors ΔP^{TCP} between the commanded position P^{TCP}_{actual} and the actual position $P^{TCP}_{commanded}$. The different positional error ΔP^{TCP} resulted in the different force profile from the Cartesian impedance controller as shown in Fig. 9c and 10c, which is explained in III-C. The contact force on the robot is further fed back to the Haptic Knob as shown in Fig. 9d and 10d. The realistic feedback force on the Haptic Knob

allows the user to command the robot with suitable force and stop upon successful insertion without damaging the slot. In addition, the insertion force from the human demonstration can be read and used for parameterization of the robot insertion program as the maximal force threshold, which is 30N for the small fuse and 40N for the large fuse.

VI. CONCLUSION

We have presented a low-cost Haptic Knob using an FOC controller, allowing intuitive position and force teach-in for industrial robots. Our proposed controlling interface for this device enables the user's efficient force and position teach-in on the robot's movement.

The application of such a device is successfully demonstrated in an industrial assembly task involving an automotive fuse box, where the precise push-down force during the insertion of a fuse is critical for successful task execution. Currently, the Haptic Knob operates as a one-dimensional device, limited to teleoperation of a single DOF on the slave device.

However, its hardware-agnostic design allows users to switch between control channels associated with different DOFs of the workcell devices. For future work, we aim to integrate multiple Haptic Knobs for multi-dimensional robot teleoperation, akin to the mechanical structure of gimbals for 3D orientation/position control of the robot TCP. Additionally, we plan to explore the use of the Haptic Knob in Virtual Reality environments to enhance robot teleoperation. We believe that the precise force and position teach-in with our Haptic Knob will also facilitate data collection for robot manipulation, which can be leveraged in imitation learning to teach robots dexterous movements, such as grasping deformable objects.

ACKNOWLEDGMENT

We would like to express our gratitude to Dong Yang for his feedback on a draft of this paper.

REFERENCES

- [1] C. Pacchierotti and D. Prattichizzo, "Cutaneous/tactile haptic feedback in robotic teleoperation: Motivation, survey, and perspectives," *IEEE Transactions on Robotics*, 2023.
- [2] C. Pacchierotti, L. Meli, F. Chinello, M. Malvezzi, and D. Prattichizzo, "Cutaneous haptic feedback to ensure the stability of robotic teleoperation systems," *The International Journal of Robotics Research*, vol. 34, no. 14, pp. 1773–1787, 2015.
- [3] D. Yang, X. Xu, M. Xiong, E. Babaians, Z. Wang, F. Meng, and E. Steinbach, "Issc: Interactive semantic shared control for haptic teleoperation," in *2023 32nd IEEE International Conference on Robot and Human Interactive Communication (RO-MAN)*. IEEE, 2023, pp. 1934–1941.
- [4] Y. Michel, R. Rahal, C. Pacchierotti, P. R. Giordano, and D. Lee, "Bilateral teleoperation with adaptive impedance control for contact tasks," *IEEE Robotics and Automation Letters*, vol. 6, no. 3, pp. 5429–5436, 2021.
- [5] T. Zhou, P. Xia, Y. Ye, and J. Du, "Embodied robot teleoperation based on high-fidelity visual-haptic simulator: Pipe-fitting example," *Journal of Construction Engineering and Management*, vol. 149, no. 12, p. 04023129, 2023.
- [6] R. Gabriel, W. Leonhard, and C. J. Nordby, "Field-oriented control of a standard ac motor using microprocessors," *IEEE Transactions on Industry Applications*, vol. IA-16, no. 2, pp. 186–192, 1980.

- [7] A. Skuric, H. S. Bank, R. Unger, O. Williams, and D. González-Reyes, "SimpleFOC: A Field Oriented Control (FOC) Library for Controlling Brushless Direct Current (BLDC) and Stepper Motors," *Journal of Open Source Software*, vol. 7, no. 74, p. 4232, June 2022. [Online]. Available: <https://joss.theoj.org/papers/10.21105/joss.04232>
- [8] A. Perzylo, I. Kessler, S. Profanter, and M. Rickert, "Toward a knowledge-based data backbone for seamless digital engineering in smart factories," in *2020 25th IEEE International Conference on Emerging Technologies and Factory Automation (ETFA)*, vol. 1. IEEE, 2020, pp. 164–171.
- [9] F. Steinmetz, A. Montebelli, and V. Kyrki, "Simultaneous kinesthetic teaching of positional and force requirements for sequential in-contact tasks," in *2015 IEEE-RAS 15th International Conference on Humanoid Robots (Humanoids)*. IEEE, 2015, pp. 202–209.
- [10] I. Jang, H. Niu, E. C. Collins, A. Weightman, J. Carrasco, and B. Lennox, "Virtual kinesthetic teaching for bimanual telemanipulation," in *2021 IEEE/SICE International Symposium on System Integration (SII)*. IEEE, 2021, pp. 120–125.
- [11] M. Sakr, M. Freeman, H. M. Van der Loos, and E. Croft, "Training human teacher to improve robot learning from demonstration: A pilot study on kinesthetic teaching," in *2020 29th IEEE International Conference on Robot and Human Interactive Communication (RO-MAN)*. IEEE, 2020, pp. 800–806.
- [12] Z. Wang, X. Xu, D. Yang, Z. Wang, S. Shtaierman, and E. Steinbach, "Haptic dataset augmentation with subjective qoe labels using conditional generative adversarial network," in *2023 IEEE/RSJ International Conference on Intelligent Robots and Systems (IROS)*. IEEE, 2023, pp. 5072–5078.
- [13] C. Chi, S. Feng, Y. Du, Z. Xu, E. Cousineau, B. Burchfiel, and S. Song, "Diffusion policy: Visuomotor policy learning via action diffusion," *arXiv preprint arXiv:2303.04137*, 2023.
- [14] L. Pagliara, E. Ferrentino, A. Chiacchio, and G. Russo, "Safe haptic teleoperations of admittance controlled robots with virtualization of the force feedback," *arXiv preprint arXiv:2404.07672*, 2024.
- [15] H. Culbertson, S. B. Schorr, and A. M. Okamura, "Haptics: The present and future of artificial touch sensation," *Annual Review of Control, Robotics, and Autonomous Systems*, vol. 1, pp. 385–409, 2018.
- [16] C. Pacchierotti, A. Tirmizi, G. Bianchini, and D. Prattichizzo, "Improving transparency in passive teleoperation by combining cutaneous and kinesthetic force feedback," in *2013 IEEE/RSJ International Conference on Intelligent Robots and Systems*. IEEE, 2013, pp. 4958–4963.
- [17] M. Rietzler, F. Geiselhart, J. Frommel, and E. Rukzio, "Conveying the perception of kinesthetic feedback in virtual reality using state-of-the-art hardware," in *Proceedings of the 2018 CHI Conference on Human Factors in Computing Systems*, 2018, pp. 1–13.
- [18] P. Weber, E. Rueckert, R. Calandra, J. Peters, and P. Beckerle, "A low-cost sensor glove with vibrotactile feedback and multiple finger joint and hand motion sensing for human-robot interaction," in *2016 25th IEEE International Symposium on Robot and Human Interactive Communication (RO-MAN)*. IEEE, 2016, pp. 99–104.
- [19] C. Yang, C. Zeng, P. Liang, Z. Li, R. Li, and C.-Y. Su, "Interface design of a physical human-robot interaction system for human impedance adaptive skill transfer," *IEEE Transactions on Automation Science and Engineering*, vol. 15, no. 1, pp. 329–340, 2017.
- [20] A. R. See, J. A. G. Choco, and K. Chandramohan, "Touch, texture and haptic feedback: a review on how we feel the world around us," *Applied Sciences*, vol. 12, no. 9, p. 4686, 2022.
- [21] V. M. Bida, D. V. Samokhvalov, and F. S. Al-Mahturi, "PMSM vector control techniques — A survey," in *2018 IEEE Conference of Russian Young Researchers in Electrical and Electronic Engineering (EIConRus)*, Jan. 2018, pp. 577–581. [Online]. Available: <https://ieeexplore.ieee.org/document/8317164>
- [22] N. Hogan, "Impedance control: An approach to manipulation," in *1984 American control conference*. IEEE, 1984, pp. 304–313.